Available online at www.sciencedirect.com
ScienceDirect
Journal of Photochemistry and Photobiology A: Chemistry 197 (2008) 81–87
Journal of Photochemistry and Photobiology A:Chemistry
www.elsevier.com/locate/jphotochem

Photodegradation of tetracycline and formation of reactive oxygen species in aqueous tetracycline solution under simulated sunlight irradiation

Yong Chen, Chun Hu *, Jiuhui Qu, Min Yang

State Key Laboratory of Environmental Aquatic Chemistry, Research Center for Eco-Environmental Sciences, Chinese Academy of Sciences, Beijing 100085, China

Received 25 September 2007; received in revised form 23 November 2007; accepted 12 December 2007
Available online 23 December 2007

Abstract

The photochemical kinetics and mechanism of the antibiotic compound tetracycline (TC) was investigated in aqueous solution under simulated sunlight irradiation. The study of the electron spin resonance revealed that the singlet oxygen ($^1O_2$) was generated and the formation rate decreased with increasing pH in illuminated TC solution. Also, it was found that the H_2O_2 was produced and increased with increasing pH under the simulated sunlight irradiation. The results verified that TC could be sunlight excited and induced the formation of reactive oxygen species. Moreover, the contributions of oxidation reaction to photodegradation of TC were clarified by the role of different radical scavengers. The kinetic model elucidated the involvement of TC photoinduced singlet oxygen on the photodegradation of TC. It was verified that the photodegradation of TC was predominantly attributed to direct photolysis. The quantum yields of direct photolysis increases with increasing pH in the range of 6.0–9.0, varying from 3.4×10^{-4} to 1.1×10^{-2}. The indirect photolysis of TC was carried out in the presence of nitrate, bicarbonate, ferric ions and humic acid (HA), respectively. The results verified that the photodegradation of tetracycline was not obviously affected by these photosensitizers except ferric ions, indicating that the direct photolysis of TC was predominant process.

Keywords: Direct photolysis; Oxidation reaction; Tetracycline; Reactive oxygen species; Self-sensitization

1. Introduction

Pharmaceuticals and personal care products (PPCPs) are now recognized as a new class of emerging pollutants and have been the subject of increasing concern and scientific interest [1,2]. Several kinds of drugs, such as antibiotics, hormones, preservatives and anesthetics, have been identified in surface water, groundwater, sewage water, and drinking water, of which antibiotics are of special concern due to their extensive use in human and veterinary medicine [3,4]. Tetracycline (TC) is one of the most frequently prescribed groups of antibiotics commonly used as therapeutics and growth promoters in husbandry, cattle, swine, poultry and fishery, with a widespread presence in surface waters [5–8].

It has been demonstrated that TC is susceptible to light sources of kinds in aqueous solution [9–12]. Nevertheless, the mechanism underlying photolysis of TC has not been well understood. During the research of phototoxicity for tetracyclines (TCs), Hasan and Khan observed the photosensitized emission of singlet oxygen in TC solution [13]. However, the later study indicated that TCs did not generate $^1O_2$ to any considerable extent [14]. Equally, the superoxide anion ($O_2^{\bullet -}$) was found in TC aqueous solution upon exposure to white light, but at the specific wavelength the generation of $O_2^{\bullet -}$ was dependent on the wavelength used [15,16]. Thus, it appeared that the generation of ROS was associated with the light sources. Until recently, however, the generation of ROS arising from irradiation of TC in natural waters has received little attention. The investigation of the involved ROS in photolysis of TC will allow us to make a mechanistic understanding of the photolysis process.

The recent studies indicated that the water hardness was an important photochemical parameter for photodegradation of TC [17], and a self-sensitization effect was suggested as one of the possible explanations for the increasing apparent rate constant at increasing initial concentration of TC. However, it was still unknown for the generation of ROS in TC aqueous solution at the natural pH since the component species of TC are pH dependent. The contributions of the possible photoinduced ROS to the

* Corresponding author. Tel.: +86 10 62849628; fax: +86 10 62923541.
E-mail address: huchun@rcees.ac.cn (C. Hu).

1010-6030/$ – see front matter © 2007 Elsevier B.V. All rights reserved.
doi:10.1016/j.jphotochem.2007.12.007

photolysis of TC was still not clear, which was very important for predicting the kinetics of TC degradation in the natural water.

In the present work, the involved ROS were studied by electron spin resonance in the photochemical reaction of TC aqueous solution under different pH conditions under simulated sunlight irradiation. Furthermore, the contributions of direct photolysis and reaction with ROS were clarified by the experiments of ROS scavengers at different pH conditions. The effects of NO_3^-, HCO_3^-, Fe(III) and humic acid (HA) on the photochemical kinetics of TC were investigated under simulated sunlight. A kinetic model for TC photodegradation was proposed based on different experiments.

2. Experimental

2.1. Materials

Tetracycline hydrochloride (98%) was purchased from the Sigma Chemical Corporation and used as received. 2,2,6,6-Tetramethylpiperidine (TEMP) (98%) was obtained from New Jersey, USA. 5,5-Dimethyl-1-pyrroline-*N*-oxide (DMPO) was purchased from the Sigma Chemical Corporation and stored at −20 °C. *N*,*N*-diethyl-1,4-phenylenediammonium sulfate (DPD) and Horseradish peroxidase (POD) were purchased from Hualin Biologic Engineering Corporation (China) and stored at 5 °C. Humic acid sodium salt was obtained from Aldrich Chemical Co. (Milwaukee, WI). Pyridine, *p*-nitroanisole (PNA), $NaHCO_3$, $NaNO_3$, $FeCl_3{\cdot}6H_2O$, *p*-quinone were supplied by Beijing Chemicals Corporation. Stock solution of TC was prepared fresh daily from the solid. All other materials were at least analytical-reagent grade.

2.2. Experimental setup

The reactor used was a 50 ml capped glass Pyrex reactor with tubing allowing bubbling gas in all experiments. The light source was a 150-W Xenon Short Arc Lamp (XBO 150 W/CR OFR) equipped with a constant current power (Zolix Corporation, Beijing). The operation current was set at 8.00 A in all experiments. The irradiation below 300 nm was cut off by the Pyrex reactor.

2.3. Analysis

Electron spin resonance (ESR) signals for singlet oxygen and superoxide anion trapped by TEMP and DMPO were obtained on a Bruker model ESP300E electron paramagnetic resonance spectrometer equipped with a Quanta-Ray Nd:YAG laser system as the irradiation light source ($\lambda = 355$ nm) at ambient temperature. The settings were center field 3482.00 G, microwave frequency 9.79 GHz and power 2.00 mW. Determination of the concentration of H_2O_2 generated in the photochemical reaction of TC under simulated sunlight irradiation was performed with a photometric method described in the literature [18].

The concentration of dissolved oxygen (DO) in the TC aqueous solution was measured with an electrochemical membrane type electrode (WTW Cellox 325) inserted vertically in the airtight reactor at 25 ± 0.5 °C.

TC and PNA were analyzed by Alliance 2695 (Waters, USA) HPLC system with 2996 Diode Array Detector and XTerra MS column (5 μm, 250 mm × 2.1 mm). The optimized mobile phase for TC was 15% methanol–25% acetonitrile–60% 0.01 M oxalic acid solution, and the flow rate was kept at 0.8 ml/min. The photodiode array detector was set at 355 nm. For PNA the mobile phase was 50% acetonitrile–50% H_2O with the flow rate 1 ml/min. The photodiode array detector was set at 300 nm.

3. Results and discussions

3.1. Effect of pH on photolysis of TC

The direct photolysis of TC was carried out at the pH range of 6.0–9.0 under simulated sunlight irradiation. The environmentally relevant quantum yields for photolysis of TC were determined using the Xenon lamp. The values were calculated from [19]

$$\phi_s = \frac{k_s}{k_a} \frac{\sum L_\lambda \varepsilon_\lambda^a}{\sum L_\lambda \varepsilon_\lambda^s} \phi_a$$

where s is the substrate, a is the actinometer, k is the rate constant for direct photolysis, L_λ values (lamp irradiance at a specific wavelength) were taken from the manufacturer, ε_λ values are the molar absorptivities of the substrate (obtained from absorbance spectra) or actinometer (tabulated values from Leifer [20]) and ϕ are the quantum yields of direct photolysis. As shown in Fig. 1, with increasing pH the light absorption of TC exhibits red shift and overlaps more with the spectrum of simulated sunlight in the long wavelength UVA region. It was found that the quantum yields for photolysis of TC increased with increasing pH at the range of 6.0–9.0 (Fig. 2). The phenomena paralleled the change of the fraction of TCH^- at different pH. At low pH, TC was fully protonated (Scheme 1). With increasing pH, the proton at O3 was released and a zwitterion was formed, which was corresponding to pK_{a1}. The second equilibrium constant of TC ($pK_{a2} = 7.68$), which is principally responsible for the fraction of TCH^-, accounted for the most environmentally relevant speciation of TC since the acid of natural waters varied generally in the range of $pK_{a2} \pm 1$. Accordingly, photodegradation of TC

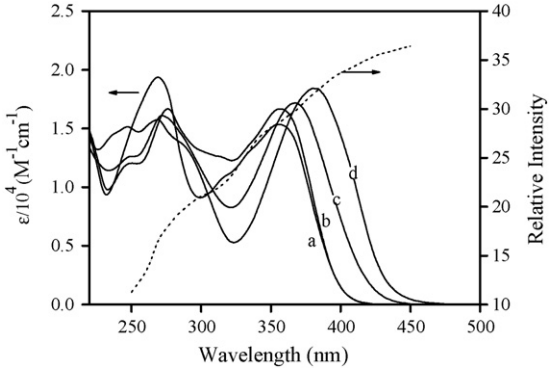

Fig. 1. Absorption spectra of different species of TC: (a) fully protonation form, TCH_3^+; (b) zwitterionic form, $TCH_2^\pm$; (c) monoanion, TCH^-; (d) dianion, TC^{2-} and the relative intensity of the light source used in this work in the region that overlaps the absorption of TC.

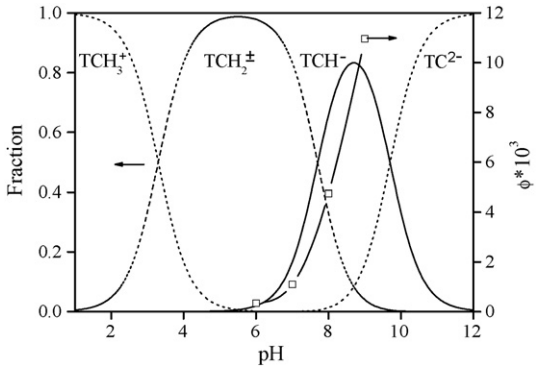

Fig. 2. Speciation-dependent quantum yields for photodegradation of TC.

in natural waters was speciation-dependent and predominantly correlated with the fraction of TCH^-.

3.2. Mechanism on photolysis of TC

To ascertain the generation of reactive oxygen species (ROS) in natural pH and study the mechanism underlying photolysis of TC, ESR experiments were performed to detect singlet oxygen ($^1O_2$) and superoxide anion ($O_2^{\bullet-}$). TEMP and DMPO were used as the probe molecules for $^1O_2$ and $O_2^{\bullet-}$, respectively. The ESR signals in Fig. 3 indicates that $^1O_2$ was generated upon irradiation of TC solutions at the pH range of 2.7–8.3. The results confirmed that $^1O_2$ could be generated by irradiation of TC not only in the fully protonated form [13], but also in the deprotonated forms of TC over the natural pH range; the results were different from the work by Miskoski et al. [14]. In our study the TC solution was excited in the ESR cavity by the third harmonic light of a pulsed Nd:YAG laser at 355 nm, which coincides with the maximum absorbance of TC, while Miskoski et al. employed 532 nm as the excited wavelength at which the TC solution shows no appreciable absorption. The production of singlet oxygen increased with decreasing pH. Accordingly, the generation of $^1O_2$ was associated with speciation of TC. This may be interpreted as an indication that TC was degraded

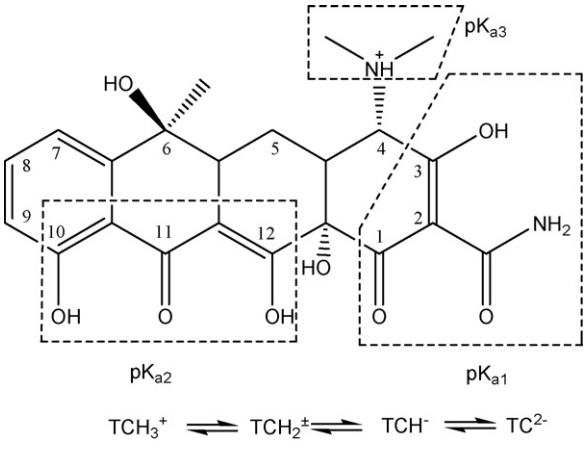

Scheme 1. Molecular structure of TC and the different protonation/deportation equilibria. The pK_a values of each acidic proton are (a) 3.3; (b) 7.68; (c) 9.7, determined by Stephens et al. [21].

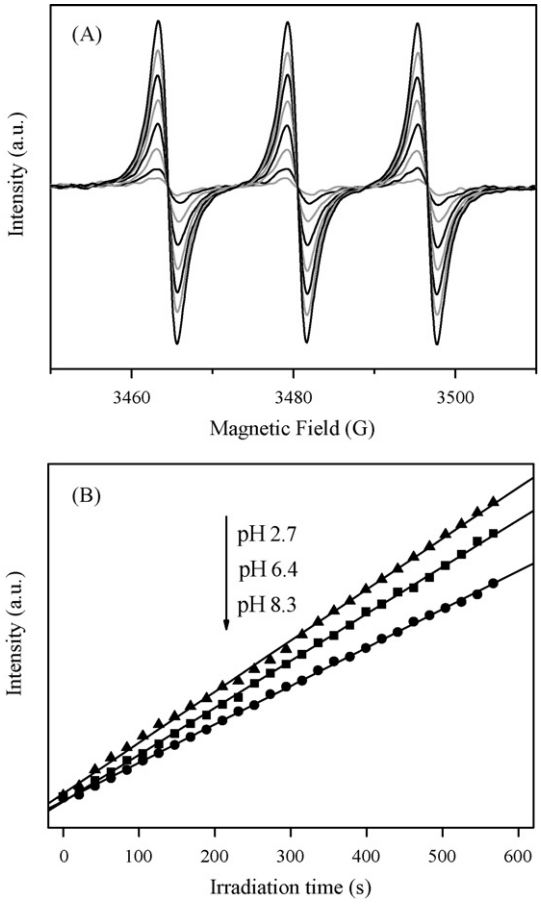

Fig. 3. ESR spectral variance of singlet oxygen with time by irradiation of TC aqueous solution in an oxygen saturated acetonitrile solution of TEMP (A) and the kinetics of ESR signal intensity of singlet oxygen at different pH (B).

more easily at higher pH instead of generating $^1O_2$. With the increasing irradiation time, the singlet oxygen increased linearly. No appreciable signal of DMPO-$O_2^{\bullet-}$ was observed. Since the oxygen quenching of the singlet or/and triplet excited states of organic molecules to yield $^1O_2$ has been extensively reported [22], it was suggested that the generation of $^1O_2$ in this photochemical reaction of TC was reasonably attributable to the same mechanism. The fluorescence emission of TC aqueous solution before and after bubbling with argon did not change appreciably (data not shown), so the singlet TC excited state was not responsible for the generation of $^1O_2$ and the quenching of triplet TC excited was suggested to yield $^1O_2$ in this system.

As one of the ROS, H_2O_2 has received little attention in the TC aqueous solution even though it has the phototoxicity [23]. For the first time the production of H_2O_2 was measured in TC aqueous solution under simulated sunlight. As shown in Fig. 4, H_2O_2 was generated in TC aqueous solution under simulated sunlight irradiation at different pH. The concentrations of H_2O_2 significantly increased with increasing pH. It was possible that H_2O_2 was generated by $O_2^{\bullet-}$ dismutation and/or the interaction between TC and the resultant $^1O_2$. To further verify this presumption, the inhibition experiments for $^1O_2$ and $O_2^{\bullet-}$ were performed by addition of NaN_3 and *p*-quinone, respectively. The results indicated that the generation of H_2O_2 was not affected

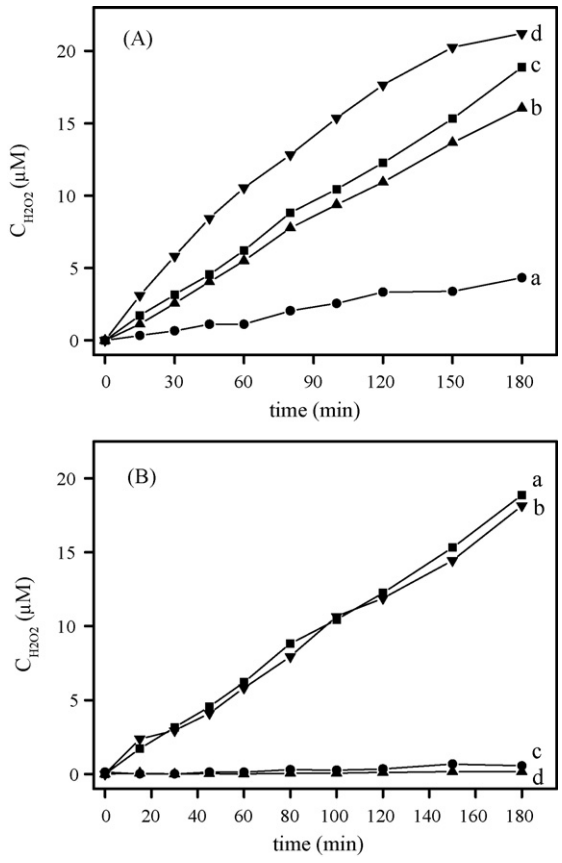

Fig. 4. Generation of H_2O_2 as a function of irradiation time in TC (200 μM) aqueous solution at pH 6.0 (a), pH 7.0 (b), pH 8.0 (c), and pH 9.0 (d) (A). Comparison of the H_2O_2 generation at pH 8.0 in the absence (a) and presence of 8 mM NaN_3 (b), N_2 atmosphere (c), and 8 mM *p*-quinone (d) (B).

obviously by NaN_3 but diminished in the presence of *p*-quinone, indicating that the generation of H_2O_2 was due to the $O_2^{\bullet-}$ dismutation. Despite failure to detect the $O_2^{\bullet-}$ at 355 nm in TC solution by ESR, the generation of H_2O_2 implied that $O_2^{\bullet-}$ was formed under simulated sunlight. This different results given by the ESR at 355 nm and the simulated sunlight at the wavelength above 300 nm suggested that the generation of $O_2^{\bullet-}$ was wavelength dependent, which was consistent with other findings that the irradiation of TC solution in the presence of DMPO at 360 nm did not generate detectable amounts of DMPO-$O_2^{\bullet-}$ while the spin adduct was readily identified at 310 nm [16].

As parallel experiments, dissolved oxygen (DO) consumption was measured in TC aqueous solution under identical conditions. Fig. 5 shows that the consumption of DO increased with increasing pH values of solution over the pH range of 6.0–9.0. The consumption of oxygen was consistent with the photodegradation rate of TC. The results indicated that oxygen was involved in the photodegradation and generation of ROS.

Fig. 6 shows the role of the resultant $^1O_2$ and $O_2^{\bullet-}$ in the photolysis of TC at pH 7.5. The addition of *p*-quinone did not obviously affect the photodegradation of TC, while NaN_3 suppressed the photolysis to the extent roughly equivalent to the absence of oxygen. However, the photolysis could only be partly suppressed, indicating the direct reaction predominantly proceeded in the system at pH 7.5.

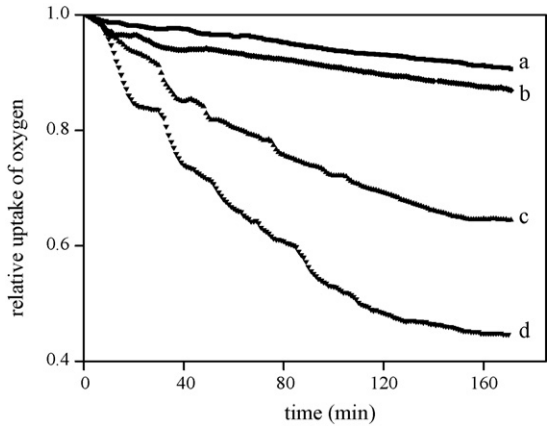

Fig. 5. Oxygen consumption as a function of irradiation time in TC (200 μM) aqueous solution at pH 6.0 (a), pH 7.0 (b), pH 8.0 (c) and pH 9.0 (d).

In photolysis reactions, excited-state photosensitizers can produce free radicals by Type I reactions and singlet oxygen by Type II reactions [24]. According to the study of ROS in TC solution, three different types of reactions may occur during TC photolysis (Scheme 2). Upon exposure to light, excited TC may undergo direct reaction (pathway a), energy transfer to generate $^1O_2$ (Type II photoprocess) or electron transfer to generate free radicals (Type I photoprocess). TC may physically quench $^1O_2$ (pathway d) or it may be oxidized either by $^1O_2$ (pathway c) or by free radicals (pathway b). The $O_2^{\bullet-}$ anions was formed in pathway b, followed by generation of H_2O_2 via $O_2^{\bullet-}$ dismutation. This pathway in the study was in agreement with the photochemically initiated photolysis of β-carotene [25].

3.3. Photolysis kinetics model

According to the pathway of TC photolysis presented in Scheme 2, a kinetic model was carried out for the further understanding of TC photodegradation at natural pH. The NaN_3 and *p*-quinone experiments suggested that $^1O_2$ was the most probable oxidant in this system. Direct reaction accounted for the

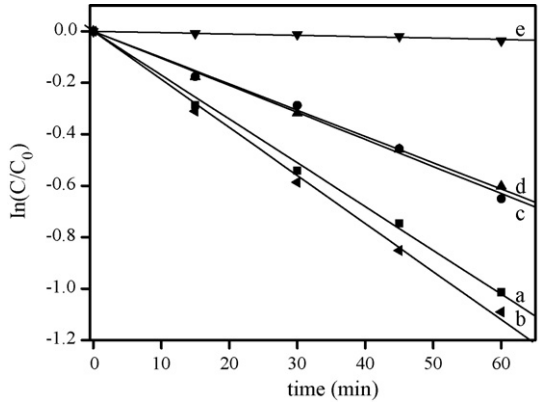

Fig. 6. Comparison of photolysis of TC (10 μM) in the absence (a) and presence of 8 mM *p*-quinone (b), N_2 atmosphere (c), 8 mM NaN_3 (d) and in the dark (e) at pH 7.5.

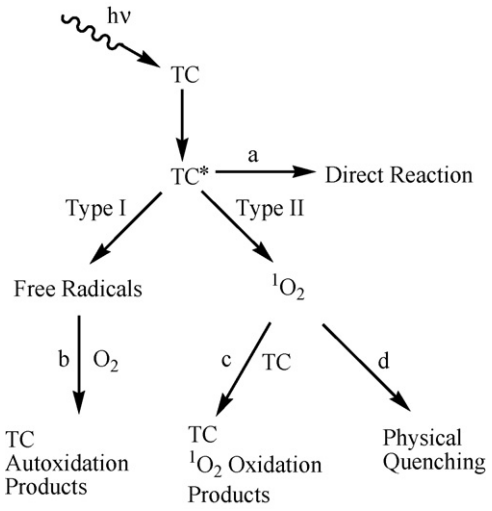

Scheme 2. The proposed pathway for photolysis of TC.

principal dissipation of TC due to the partly inhibition of the photolysis by addition of $^1O_2$ scavenger. Thus, a simplified reaction scheme can be used to describe the system [26,27]:

$$TC \xrightarrow{h\nu, I_a, \phi} TC^*(\text{triplet state}) \quad (1)$$

$$TC^* + {}^3O_2 \xrightarrow{k_T} TC + {}^1O_2 \quad (2)$$

$${}^1O_2 \xrightarrow{k_d} {}^3O_2 \quad (3)$$

$${}^1O_2 + TC \xrightarrow{k_r} \text{products} \quad (4)$$

$${}^1O_2 + TC \xrightarrow{k_q} {}^3O_2 + TC \quad (5)$$

$$TC^* \xrightarrow{k_p} \text{products} \quad (6)$$

where I_a is the rate of light absorption by TC, ϕ is the quantum yield for TC^*, k_T is the second-order rate constant between TC^* and $^3O_2$, k_d is the first-order rate constant for physical quenching of $^1O_2$ by water, k_r is the second-order rate constant for the chemical reaction between $^1O_2$ and TC, k_q is the second-order rate constant for physical quenching of $^1O_2$ by genetic $^1O_2$ quenchers Q (a term including TC), and k_p is the direct photodegradation rate constant of TC.

The steady-state approximation for triplet state of TC is:

$$\frac{d[TC^*]_{ss}}{dt} = \phi I_a - k_T[{}^3O_2][TC^*]_{ss} - k_p[TC^*]_{ss} = 0 \quad (7)$$

Rearranging Eq. (7) yields

$$[TC^*]_{ss} = \frac{\phi I_a}{k_p + k_T[{}^3O_2]} \quad (8)$$

The steady-state approximation for $^1O_2$ is

$$\frac{d[{}^1O_2]_{ss}}{dt} = k_T[{}^3O_2][TC^*]_{ss} - k_d[{}^1O_2]_{ss} - (k_r + k_q)[TC][{}^1O_2]_{ss} = 0 \quad (9)$$

Rearranging Eq. (9) yields

$$[{}^1O_2]_{ss} = \frac{k_T[{}^3O_2][TC^*]_{ss}}{k_d + (k_r + k_q)[TC]} = \frac{\phi I_a k_T[{}^3O_2]}{\{k_p + k_T[{}^3O_2]\}\{k_d + (k_r + k_q)[TC]\}} \quad (10)$$

The value of k_d for $^1O_2$ is $2.5 \times 10^5\ s^{-1}$ [28]. The initial concentration of TC in this work was 10 μM, so k_d will be much greater than $(k_r + k_q)[TC]$ as long as $k_r + k_q$ does not approach its diffusion-controlled limit. Assuming this to be the case, Eq. (10) can be simplified to

$$[{}^1O_2]_{ss} = \frac{\phi I_a k_T[{}^3O_2]}{k_d\{k_p + k_T[{}^3O_2]\}} \quad (11)$$

According to the Beer–Lambert law,

$$I_a = I_0(1 - e^{-\varepsilon b[TC]}) \quad (12)$$

For the low concentration of TC, $\varepsilon b[TC] \ll 1$, Eq. (12) can be simplified to

$$I_a = I_0 \varepsilon b[TC] \quad (13)$$

According to Eqs. (4) and (6), the photodegradation rate of TC is shown as follow:

$$-\frac{d[TC]}{dt} = k_r[{}^1O_2]_{ss}[TC] + k_p[TC^*]_{ss} \quad (14)$$

Substituting Eqs. (8), (11) and (13) into Eq. (14) yields

$$-\frac{d[TC]}{dt} = \frac{\phi I_0 \varepsilon b[TC]}{k_p + k_T[{}^3O_2]}\left\{\frac{k_T k_r[{}^3O_2]}{k_d}[TC] + k_p\right\} \quad (15)$$

Rearranging Eq. (15) yields

$$-\frac{1}{[TC]}\frac{d[TC]}{dt} = \frac{\phi I_0 \varepsilon b}{k_p + k_T[{}^3O_2]}\left\{\frac{k_T k_r[{}^3O_2]}{k_d}[TC] + k_p\right\} \quad (16)$$

In this study, the various initial concentrations of TC were the function of the corresponding initial photodegradation rate. The results are presented in Fig. 7. The data was in good accordance with Eq. (16). The y-intercepts of these lines at different pH

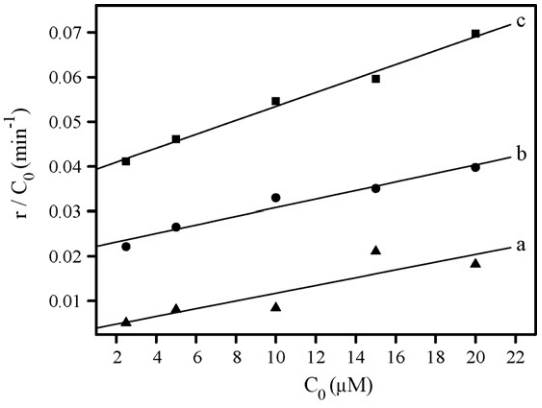

Fig. 7. The initial rate of TC with various initial concentrations at pH 6.5 (a), pH 8.0 (b) and pH 9.0 (c).

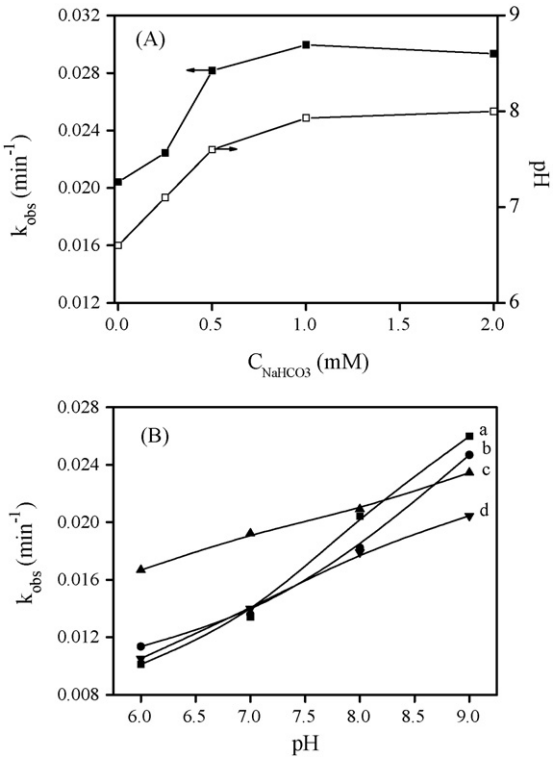

Fig. 8. Effect of HCO_3^- on the pseudo-first-order rate constant k_{obs} for photodegradation of TC (10 μM) at pH 8.0 (A) and comparison of k_{obs} for photodegradation of TC (10 μM) in the absence (a) and presence of 1.0 mM NO_3^- (b),10 μM Fe^{3+} (c) and 5.0 mg L^{-1} HA (d) at various pH (B).

are the rate constants of the direct photodegradation. The ratio $k_T k_r[^3O_2]/k_d k_p$ can be estimated to be 0.028, 0.045 and 0.041 at pH 6.5, 8.0 and 9.0, respectively. The model indicated that the direct photodegradation contributed to the principal dissipation of TC at low pH with little contribution of self-sensitization effect. The Type II photoprocess became increasingly significant with increasing pH at the pH range of 6.5–9.0. The good correlations between the experimental data and the models verified that the direct photolysis and Type II photoprocess coexist during the photodegradation of TC.

3.4. Indirect photolysis kinetics

The kinetics of TC photodegradation coupled with HCO_3^-, NO_3^-, Fe^{3+} and HA were examined. As shown in Fig. 8A, both the photodegradation rate of TC and the final pH of reaction solution increased by the addition of HCO_3^-, and tended to certain stable value with increasing concentration of bicarbonate. Since the photodegradation of TC increased with increasing pH, the results suggested that the effect of HCO_3^- was attributed to its adjusting role of pH. With increasing concentration of HCO_3^-, the buffer capacity was enough to keep the constant pH of TC aqueous solution. Thus, the photodegradation rate tended to stability. The results suggested that HCO_3^- did not significantly affect the photodegradation of TC. The effect of NO_3^-, Fe^{3+} and HA on photodegradation of TC is presented in Fig. 8B. The NO_3^- is photochemical reactive and the photolysis of NO_3^- to produce NO_2^- and $HO^\bullet$ is well known [29,30]. However, in this experiment, the addition of NO_3^- did not affect the TC photodegradation rate over the pH range 6.0–9.0. For the photodegradation of TC, the Fe^{3+} exhibited the different role at various pH. TC photodegradation was obviously increased in the presence of Fe^{3+} at the pH range of 6.0–7.0. With the increasing pH of TC aqueous solution, the enhancement diminished at pH 8.0 and even an inhibition effect was observed at pH 9.0. It has been established that TC forms reversible complexes with Mn^{2+}, Zn^{2+}, Mg^{2+} and Ca^{2+} and these TC-metal ions complexes exhibited different photoreactivity from the TC itself [31,32]. In contrast to these divalent metals, the ferric ions not only bind strongly to TC and affect the photolysis but also are photoreactive species. Thus, it was expected that in the Fe(III)–TC complex the Fe(III) undergoes photoreduction, which is accompanied by oxidation of the TC organic ligand. It is well known that $FeOH^{2+}$ in aqueous solution undergoes a photoredox process to generate Fe(II) and hydroxyl radicals [33–35]. The previous research showed that the photoactivity of $FeOH^{2+}$ in aqueous solution was significantly inhibited at pH > 5.0. Hence, the photolysis of TC in the presence of Fe(III) was presumably attributed to the complexation behavior and the possible oxidation as the organic ligand over the pH range of 6.0–8.0. At pH 9.0, the addition of Fe(III) inhibited the photolysis. This was due to the precipitation of ferric ion at the strong alkaline pH instead of complexation with TC. With the addition of HA, the photodegradation of TC was negligibly affected at pH 6.0–7.0, while it was suppressed at pH 8.0–9.0. The role of HA was a paradox since on the one hand it absorbs the incident light and decreases the light absorption of TC aqueous solution, but on the other hand the triplet HA excited state, the HA photoinduced $^1O_2$ and $O_2^{\bullet-}$ are the photoreactive species exhibiting effect on photolysis of TC. Accordingly, based on the different experiments, it was found that the main photosensitizers NO_3^- and HA had no significant influence on the photodegradation rate of TC. This implied that the direct photolysis of TC was the predominant reaction in the natural water.

4. Conclusion

The measurements of the electron spin resonance and photometric method revealed that $^1O_2$ and H_2O_2 were generated in the TC solution under simulated sunlight irradiation over the natural pH range. Both the photolysis and photoproduction of these ROS are dependent on the speciation of TC. The photodegradation of TC were attributable to direction action of the excited states and the self-sensitization. The photolysis of TC was unaffected obviously in the natural pH in the presence of nitrate, bicarbonate and HA, indicating the direct photolysis of TC was possibly the predominant photochemical reaction process. The ferric ions exhibit enhancement for the photolysis over the pH range of 6.0–8.0, but an inhibition is observed at pH 9.0.

Acknowledgement

This work was supported by the National 863 Project of China (Grant No. 2006AA06Z304) and Natural Sciences Foundation

of China (Grant No. 50621804). Authors gratefully acknowledge the reviewers of this article.

References

[1] C.G. Daughton, T.A. Ternes, Environ. Health Perspect. 107 (1999) 07–938.
[2] I. Dalmázio, M.O. Almeida, R. Augusti, T.M.A. Alves, J. Am. Soc. Mass Spectrom. 18 (2007) 679–687.
[3] I.R. Bautitz, R.F.P. Nogueira, J. Photochem. Photobiol. A: Chem. 187 (2007) 33–39.
[4] C. Reyes, J. Fernández, J. Freer, M.A. Mondaca, C. Zaror, S. Malato, H.D. Mansilla, J. Photochem. Photobiol. A: Chem. 184 (2006) 141–146.
[5] M.A. Khan, J. Mustafa, J. Musarrat, Mutat. Res. Fund. Mol. M. 525 (2003) 109–119.
[6] H. Sanderson, F. Ingerslev, R.A. Brain, B. Halling-Sørensen, J.K. Bestari, C.J. Wilson, D.J. Johnson, K.R. Solomon, Chemosphere 60 (2005) 619–629.
[7] J.W. Fritz, Y. Zuo, Food Chem. 105 (2007) 1297–1301.
[8] Y. Zuo, K. Zhang, Y. Deng, Chemosphere 63 (2006) 1583–1590.
[9] D.E. Moore, M.P. Fallon, C.D. Burt, Int. J. Pharmacol. 14 (1983) 133–142.
[10] H. Oka, Y. Ikai, N. Kawamura, M. Yamada, K. Harada, S. Ito, M. Suzuki, J. Agric. Food Chem. 37 (1989) 226–231.
[11] M.M. Beliakova, S.I. Bessonov, B.M. Sergeyev, I.G. Smirnova, E.N. Dobrov, A.M. Kopylov, Biochemistry (Mosc) 68 (2003) 182–187.
[12] B. Verma, J.V. Headley, R.D. Robarts, J. Environ. Sci. Health Part A: Toxic Hazard. Subst. Environ. Eng. 42 (2007) 109–117.
[13] T. Hasan, A.U. Khan, Proc. Natl. Acad. Sci. U.S.A. 83 (1986) 4604–4606.
[14] S. Miskoski, E. Sánchez, M. Garavano, M. López, A.T. Soltermann, N.A. García, J. Photochem. Photobiol. B: Biol. 43 (1998) 164–171.
[15] M.A. Khan, J. Musarrat, Comp. Biochem. Physiol. Part C 131 (2002) 439–446.
[16] A.S.W. Li, H.P. Roethling, K.B. Cummings, C. Chignell, Biochem. Biophys. Res. Commun. 146 (1987) 1191–1195.
[17] J.J. Werner, W.A. Arnold, K. Mcneill, Environ. Sci. Technol. 40 (2006) 7236–7241.
[18] H. Bader, V. Sturzenegger, J. Hoigné, Water Res. 22 (1988) l109–l110.
[19] D. Dulin, T. Mill, Environ. Sci. Technol. 16 (1982) 815–820.
[20] A. Leifer, The Kinetics of Environmental Aquatic Photochemistry: Theory and Practice, American Chemical Society, Washington, DC, 1988.
[21] C.R. Stephens, K. Murai, K.J. Brunings, R.B. Woodward, J. Am. Chem. Soc. 78 (1956) 4155–4158.
[22] W.M. Nau, J.C. Scaiano, J. Phys. Chem. 100 (1996) 11360–11367.
[23] K. Skrivanova, J. Skorpikova, J. Svihalek, V. Mornstein, R. Janisch, J. Photochem. Photobiol. B: Biol. 85 (2006) 150–154.
[24] C.S. Foote, Quenching of singlet oxygen, in: H.H. Wasserman, R.W. Murray (Eds.), Singlet Oxygen, Academic Press, New York, 1979, pp. 139–171.
[25] S.P. Stratton, W.H. Schaefer, D.C. Liebler, Chem. Res. Toxicol. 6 (1993) 542–547.
[26] C.S. Foote, Acc. Chem. Res. 1 (1968) 104–110.
[27] L. Kong, J.L. Ferry, Environ. Sci. Technol. 37 (2003) 4894–4900.
[28] M.A.J. Rodgers, P.T. Snowden, J. Am. Chem. Soc. 104 (1982) 5541–5543.
[29] O.C. Zafiriou, J. Geophys. Res. 79 (1974) 4491–4497.
[30] Y. Zuo, Y. Deng, Chemosphere 36 (1998) 181–188.
[31] H. Morrison, G. Olack, C. Xiao, J. Am. Chem. Soc. 113 (1991) 8110–8118.
[32] M.G.A. Wahed, M. Ayad, R.E. Sheikh, Anal. Lett. 17 (1984) 413–422.
[33] Y. Deng, H. Chen, T. Wu, M. Krzyaniak, A. Wellons, D. Bolla, K. Douglas, Y. Zuo, Atmos. Environ. 40 (2006) 3665–3676.
[34] I.P. Pozdnyakov, E.M. Glebov, V.F. Plyusnin, V.P. Grivin, Yu.V. Ivanov, D.Y. Vorobyev, N.M. Bazhin, Pure Appl. Chem. 72 (2000) 2187–2197.
[35] F. Wu, N.S. Deng, Chemosphere 41 (2000) 1137–1147.